scientific reports

Check for updates

OPEN

Structural, surface, and theoretical investigation of hydrophobic-modified nanodiamond powders

Nazerke Kydyrbay[1], Mergen Zhazitov[1], Muhammad Abdullah[1], Tolagay Duisebayev[1], Yerbolat Tezekbay[1], Anuar Aldongarov[3], Mirat Karibayev[1,2], Nurxat Nuraje[1,2] & Olzat Toktarbaiuly[1]✉

Nanodiamonds (NDs) have received much attention in science and technology due to their superior structural and functional characteristics. In this study, NDs were successfully functionalized with Triethoxy(octyl)silane (TREOS) to make them superhydrophobic. Surface functionalization was carried out through hydrolysis and condensation reactions to create stable Si–O–C and Si–O–Si bonds. Characterization techniques like Raman spectroscopy, XRD, SEM, FTIR, and water contact angle measurements confirmed the structural integrity and efficient functionalization of the functionalized NDs. The observed superhydrophobicity with a 151° contact angle is understandable based on both silane functionalization and nanoscale surface roughness. These observations suggest the prospects of TREOS-modified NDs for use in waterproof coatings, self-cleaning surfaces, and anti-corrosion materials. Furthermore, the excellent dispersion of hydrophobic NDs in nonpolar solvents reveals that they can be applied in lubrication and anti-wear. Future efforts would be the further improvement of ND surface modification and its application in practical products, e.g., protective coatings, biomedical devices, and high-performance nanocomposites.

Nanodiamonds (NDs) are a newly emerging family of carbon nanomaterials characterized by their remarkable mechanical, optical, and chemical properties. Their structure comprises a sp^3-hybridized diamond core and a surface enriched with sp^2-hybridized carbon and functional groups, which makes NDs extremely biocompatible, non-toxic, and exhibit superior thermal conductivity[1–4]. These attributes combined with homogenous morphology and isomorphic shape highlighted NDs as promising materials for various technological applications. However, pristine NDs tend to undergo agglomeration through enhanced interparticle interactions, which hinder their performance across most applications. Aggregation is therefore a major problem that demands efficient surface functionalization to enhance ND dispersion and expand their application area in various fields. The structural composition of NDs typically consists of a diamond crystalline core covered with an amorphous carbon outer shell comprising sp^3-hybridized carbon and graphene-like carbon structures. With particle sizes typically smaller than 100 nm, ND films possess outstanding features of high hardness, low surface roughness, and low stress[5,6]. These outstanding mechanical properties result from their unique structural organization, facilitated by diamond's inherent hardness and making the NDs applicable in applications such as cutting materials, hard coatings, and abrasives[7]. Moreover, heir addition to metal composites enhances strength, hardness, and wear resistance[8], thereby proving that they can serve as reinforcement materials for other matrices in several applications.

Different synthesis methods have been modified for synthesizing NDs, including high-pressure high-temperature (HPHT) synthesis, chemical vapor deposition (CVD), laser ablation, and detonation techniques. Of these, HPHT and detonation techniques are economical and most frequently used[9]. All synthesis pathways yield NDs with varying properties, which can be tailored to specific applications. The substantial optical bandgap of 5.5 eV offers ultraviolet to infrared transparency[10], making NDs particularly ideal for optical applications. Furthermore, their high refractive index makes them ideal in polymer coatings and other related optical materials.

Surface functionalization, and more so hydrophobic functionalization, has provided the main approach to diversify ND applications to include waterproof coatings, icephobic surfaces, and corrosion barriers. Hydrophobic modification significantly alters the surface properties of NDs, lowering their particle sizes in

[1]Renewable Energy Laboratory, National Laboratory Astana (NLA), Nazarbayev University, Astana 010000, Kazakhstan. [2]Department of Chemical and Materials Engineering, School of Engineering and Digital Science, Nazarbayev University, Astana 010000, Kazakhstan. [3]Department of Technical Physics, L.N. Gumilyov Eurasian National University, Astana 010000, Kazakhstan. ✉email: toktarbo@tcd.ie

organic solvents such as tetrahydrofuran and enhancing compatibility with polymeric matrices[11]. The physical characteristics of NDs are highly size-dependent, with smaller particles possessing higher surface energy, making them more reactive and functionalized. This size-dependent effect is a key factor in deciding the efficacy of surface modification methods and subsequently the functionality of surface-modified NDs for a variety of applications.

Superhydrophobic ND coatings have also been synthesized with utmost attention on their enhanced mechanical and electrical properties along with water-repellent character. These functional materials hold great promise for applications in infrastructure protection, road construction, textile industry, and oil recovery by improving durability, reducing maintenance, and enhancing surface functionalities[12–16]. For instance, there is recent confirmation that superhydrophobic coatings can significantly enhance the durability of cement surfaces for road construction[15], with similar methods showing promising results in the development of self-cleaning building materials[16] and water-repellent microfiber applications[14].

Various strategies have been pursued for the modification of ND surfaces. Liu et al. attached poly (L-lactic acid) and poly(ε-caprolactone) onto NDs covalently using hydroxyl-initiated ring-opening polymerization to enhance dispersion[17]. The method yielded biodegradable ND-polymer composites with high compatibility in various media. Barras et al. employed surface functionalization using dopamine derivatives, providing other functional platforms for further modification[18]. This approach leveraged the face stability of catechol chemistry to graft diverse functional groups onto the ND surface. Zhang et al. grafted deoxyribonucleic acid (DNA) onto the NDs for application in gene delivery, with new progress in the research field of nanomedicine[19]. These DNA-modified NDs showed promising performance as gene delivery vectors, suggesting enormous potential for biomedical applications.

Some recent studies on making superhydrophobic ND coatings via bias-assisted reactive ion etching in hydrogen/argon plasmas[20] have been conducted. The plasma process creates nanoscale roughness on the ND surface, enhancing its inherent properties and resulting in superhydrophobic behavior. Superhydrophobic nanocomposite coatings composed of nanodiamonds and siloxane-acrylic resins have been fabricated by spray coating by other groups with excellent water repellency, enhanced anti-icing performance, good antibacterial adhesion prevention, and corrosion protection[12,21]. Researchers have also examined ND-modified chromium coatings with enhanced wear resistance[22]. ND-sensitive coatings have also been prepared for chemical vapor sensing applications, where layer-by-layer deposition techniques improve sensor sensitivity[23]. Such examples illustrate the diverse ways of preparing hydrophobic ND surfaces and show the growing research interest in this regard.

Earlier studies have provided the potential for creating superhydrophobic nanodiamond-based coatings through varying approaches, like incorporating nanodiamonds into siloxane-acrylic resin matrices[21]. The specific use of triethoxy(octyl) silane (TREOS) as a silane coupling agent for surface direct functionalization of NDs to create superhydrophobicity is a novel approach with certain unique advantages. Unlike previous methods that primarily incorporate unmodified NDs into hydrophobic matrices, our approach focuses on the direct modification of the ND surface with TREOS, creating intrinsically hydrophobic nanoparticles that can subsequently be incorporated into various polymer systems.

Silane coupling agents like TREOS offer the following important advantages for ND modification: simple single-step processing, formation of stable covalent Si–O–C linkages with the ND surface, improved thermal stability compared to polymer coatings, and the ability to precisely control hydrophobicity by adjusting reaction conditions. Large surface area, excellent mechanical integrity, and surface chemistry that can be engineered using NDs enable them to be used as polymer fillers to enhance material properties such as mechanical strength, optical clarity, and thermal conductivity[10]. The TREOS modification process specifically provides better interfacial interaction between NDs and hydrophobic polymer matrices necessary for the design of high-performance composite materials with better dispersion stability.

Although NDs have been promising in other applications such as energy storage systems[24–27], where they are employed as electrode materials for batteries and supercapacitors owing to their high electrochemical stability, their potential in superhydrophobic coatings remains largely unexploited. Their application in electrochemical sensors[28–31] has resulted in greater sensitivity and stability, whereas in photovoltaic devices[32,33], their application resulted in increased light scattering and current density in dye-sensitized solar cells. ND-drug conjugates, in biomedical engineering[30], have proven to be promising for cancer treatment, such that ND-doxorubicin complexes effectively restricted drug circulation half-life but boosted therapeutic efficiency. Nonetheless, synthesis of superhydrophobic ND-polymer composites by silane coupling agents is a missing research area that is worth systematic study.

This work covers the gap by systematically examining the triethoxy(octyl) silane modification of NDs and characterizing the resultant materials by employing advanced spectroscopic and microscopic methods. We apply Raman microscopy to analyze the structural modification of the carbon structure[6], providing us with signs of the sp^3/sp^2 carbon ratio and structural integrity after alteration. Fourier-transform infrared spectroscopy (FTIR) is employed to confirm successful surface functionalization through identification of specific functional groups for TREOS attachment. Scanning electron microscopy (SEM) examines morphological transformation and aggregate development, while X-ray diffraction (XRD) examines crystalline features and potential structural transformation induced by the modification process. Quantitative water contact angle measurements provide measurement of the resulting hydrophobicity, which provides a direct correlation between surface modification and functional ability.

Our approach takes advantage of existing knowledge of ND synthesis and modification methods but with specific emphasis placed on enhancing surface hydrophobicity through the utilization of silane coupling. The grafting-to approach employed here gives a straightforward and scalable pathway to ND functionalization, which could lead to industrialization. The above comprehensive characterizations provide valuable information

on the structure and surface chemistry of hydrophobic-modified NDs, and they pave the way for their broader applications for advanced material science with special interest in superhydrophobic coatings and surfaces for application in construction materials[13,16], microfiber technologies[14], and road engineering[15]. The results of this study contribute to the burgeoning literature on functional nanomaterials and present practical strategies for synthesizing high-performance superhydrophobic surfaces with functionalized nanodiamonds.

Materials and methods

Chemicals

Diamond Nanoparticles (Sigma-Aldrich, nano powder spherical, 5–15 nm particle size), Triethoxy (octyl)silane (TREOS) (Sigma-Aldrich, technical, 97%, MW: 276.49 g/mol), acetic acid, ethanol (95% purity), DI water.

Hydrophobic modification of nanodiamonds (NDs)

ND powders were chemically modified with TREOS to render them hydrophobic. Initially, the pH of 3 mL of deionized (DI) water was adjusted to 4–5 using acetic acid under agitation. TREOS were initially prepared in ethanol solution at 1:50 concentration and added to the stirred mixture. Exactly 0.02 mL of TREOS was dissolved in 1 mL of ethanol before introduction into the reaction. After 5 min, 0.01 g NDs were added to the solution and agitated constantly at 50 °C for 2 h for assisting the process of surface modification. After that, the reaction mixture was centrifuged to separate the functionalized NDs. Finally, the final product was dried at 60 °C for 24 h to remove surplus solvents and complete the hydrophobic modification.

Characterization techniques

The sample morphology was examined using a ZEISS Crossbeam 540 scanning electron microscope (Oberkochen, Germany). High-resolution SEM imaging was conducted at 15 kV accelerating voltage with a 5 nm spot size. Charging effects were reduced by coating the samples with a thin layer of gold before observation. Raman spectroscopy was performed on a LabRAM (Horiba) Raman spectrometer (France SAS) with a blue 532 nm laser of 10 mW power and 1 µm spot size for high spatial resolution. Water contact angle (WCA) was determined using a Data physics OCA 15 Pro goniometer (Filderstadt, Germany), and a 5 µL water droplet was placed on the surface of the sample and its profile was analyzed to determine the static contact angle. The final WCA value was obtained by averaging three separate measurements. Infrared spectra were obtained on a Nicolet iS10 FTIR spectrometer (Thermo Fisher Scientific, Waltham, MA, USA) at 4000 cm^{-1} and 400 cm^{-1} with a resolution of 4 cm^{-1}. Each spectrum was a mean of 64 scans in air as reference background for accurate spectra. X-ray diffraction analysis was performed on a Rigaku SmartLab® X-ray diffraction instrument (Tokyo, Japan) with Cu-Kα radiation ($\lambda = 1.5406$ Å). It scanned an angular range of 10° to 60° at a rate of 5° min^{-1} in 60 s to enable the crystalline structure and phase composition of the samples to be assessed.

DFT calculations

In this study, representative segments of both unfunctionalized and functionalized nanodiamonds (NDs) were selected as model systems for Density Functional Theory (DFT) calculations (Fig. 1). The structural models were constructed based on previously reported experimental findings, ensuring realistic and relevant system configurations[34]. In the selected cluster, the ND core was primarily composed of sp^3-hybridized carbon atoms, and the surface was terminated with hydrogen atoms to mimic experimental conditions. Functional groups such as hydroxyl (–OH) and triethoxysilane (TREOS) moieties were introduced to simulate functionalized surfaces. DFT simulations were performed on three systems: (i) a representative unfunctionalized ND segment, (ii) a functionalized ND model, and (iii) a functionalized ND model with an explicitly added water molecule[34]. This stepwise modeling enabled comparative analysis of the structural and electronic changes induced by functionalization and hydration.

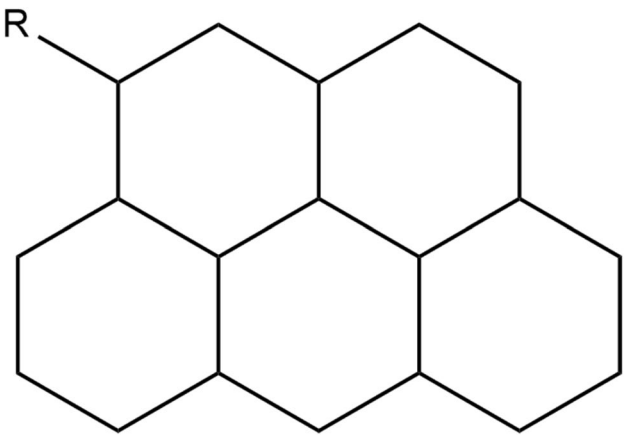

Fig. 1. Schematic representation of ND crystal structure showing several functional moieties where R is OH, and TREOS respectively[34].

Computational details

All DFT calculations were performed using the GAUSSIAN09 software package[35]. The 6–311 + + G (d, p) basis set was employed for all atoms to ensure high accuracy. Tight self-consistent field (SCF) convergence criteria of 10^{-8} a.u. were applied for electronic energy convergence to enhance the reliability of the results.

The optimized geometries were verified as true minimum by performing analytical second derivative (vibrational frequency) calculations. Further analyses were conducted using GAUSSVIEW, MULTIWFN[36], and VMD[37], including:

1. Molecular electrostatic potential (MEP) mapping,
2. Non-covalent interaction (NCI) visualization,
3. Reduced density gradient (RDG) analysis,
4. Topological critical point (CP) identification based on the Quantum Theory of Atoms in Molecules (QTAIM),
5. Evaluation of key bond distances and structural snapshots.

Structural optimizations were carried out using the B3LYP exchange–correlation functional with Grimme's D3 dispersion correction[38] to account for van der Waals interactions. These detailed DFT calculations provide critical molecular-level insights into the behavior and stability of ND-based superhydrophobic coatings, shedding light on their potential applications in extreme water-resistant technologies.

Results and discussion

Surface functionalization of NDs by TREOS is carried out through a two-step reaction process of hydrolysis and condensation to render them hydrophobic. TREOS is hydrolyzed initially in the ethanol/water solvent in which its ethoxy groups are oxidized by water to produce silanol (–SiOH) groups with ethanol as a byproduct. These silanol groups subsequently condense with surface-attached hydroxyl (–OH) and carboxyl (–COOH) functional groups on the ND surface and covalently attach via Si–O–C or Si–O–Si linkages. This reaction grafted the silane onto the NDs, yielding a stable surface modification. The reaction scheme is presented in (Fig. 2). Some of the silanol groups also self-condense, creating Si–O–Si networks that contribute to further improvement of the coating. The most significant outcome of this process is exposing long octyl ($-C_8H_{17}$) chains at the ND surface, which significantly lower surface energy and impart strong hydrophobicity. Therefore, the TREOS functionalized NDs are hydrophobic and dispersed in organic solvents more readily and are very suitable for waterproof coatings, self-cleaning materials, and corrosion-resistance applications. This functionalization is also complemented by investigations of hydrophobic films using TREOS that exhibit the formation of hydrophobic films on substrates through the same condensation and hydrolysis reactions[39]. Further research on the hydrolysis and condensation behavior of silane coupling agents provides insight into the mechanisms and kinetics of these reactions[40].

Raman spectra

The Raman spectra of both unmodified and modified NDs, presented in (Fig. 3a), highlights distinct peaks that confirm their structural characteristics. In the unmodified sample, a notable peak at 1337 cm^{-1} appears, which is a well-established marker of the sp^3-hybridized carbon framework found in diamond[41]. This peak corresponds to the optical phonon mode, confirming the presence of a crystalline ND core. In addition, wide peaks at 1600–1700 cm^{-1} (G-band) and 1200 cm^{-1} (D-band) confirm the presence of graphene-like sp^2 carbon impurities.

In the modified sample, the emergence of the G-band at higher than1600 cm^{-1} confirms that surface modifications have included sp^2 chain-like structures, shifting the vibrational mode. This change could be attributed to passivation of the surface, functionalization, or increased disorder in the carbon skeleton, in accordance with previous work on ND transformation mechanisms[42]. During surface modification, a considerable loss of peak intensity is observed, indicating changes in surface chemistry—due to passivation or functionalization—which quenches resonance effects. All these changes aside, the underlying sp^3-carbon backbone remains unchanged because the 1337 cm^{-1} band persists. These findings are consistent with previous reports, wherein functionalization alters the surface composition but does not dismantle the diamond structure in the bulk[6,43].

XRD analysis

The XRD pattern of the NDs, shown in (Fig. 3b), confirms their crystallinity by the observation of sharp diffraction peaks. A broad peak at approximately 43.5° (2θ) can be assigned to the (111) plane of the cubic diamond structure, which is characteristic of NDs and indicates a highly ordered sp^3-hybridized carbon

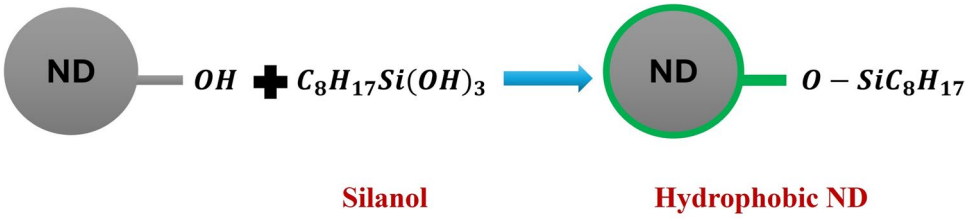

Fig. 2. Modification process of NDs by TREOS.

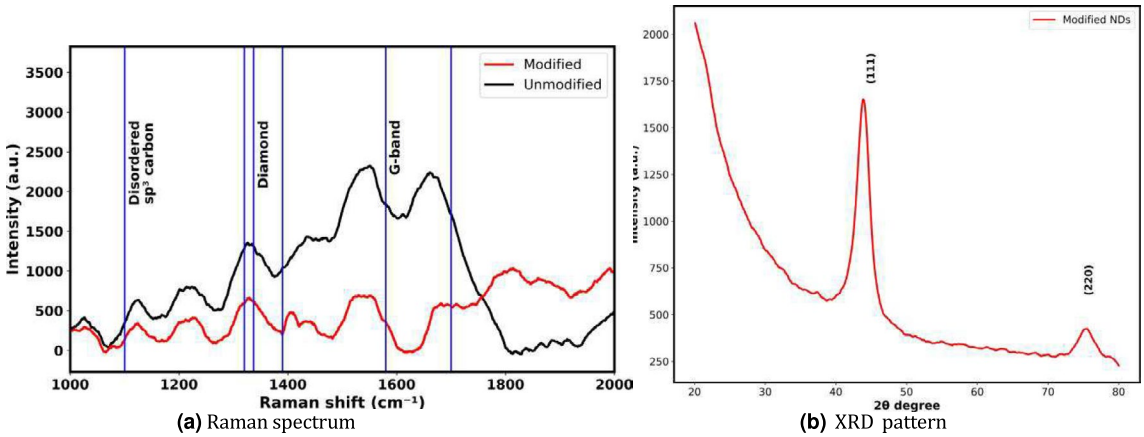

(a) Raman spectrum **(b)** XRD pattern

Fig. 3. (**a**) Raman and (**b**) XRD patterns of the TREOS modified NDs.

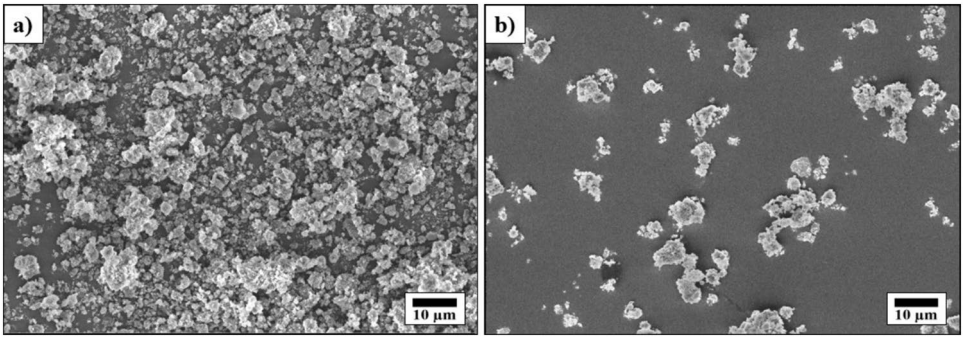

Fig. 4. SEM pictures of NDs (**a**) before and (**b**) after surface modification.

structure. Also, a small peak at 75° (2*θ*) is attributed to the (220) plane, which further supports the presence of the diamond phase. The width of these peaks is indicative of nanoscale crystallite size, consistent with the nature of NDs. There is also a broad background signal at lower angles, which may be attributed to disordered carbon or an amorphous phase, frequently assigned to surface defects or graphitic layers. This finding attributed to disordered carbon or an amorphous phase, frequently assigned to surface defects or graphitic layers. This finding additional diffraction peak confirms that the sample consists of pure ND free from any detectable impurity or secondary phases, thereby establishing its structural purity.

Surface morphology

Figure 4 illustrates the surface morphology of nanodiamonds (NDs) before and after surface modification with triethoxy(octyl)silane, as observed via SEM. In the unmodified sample (Fig. 4a), the NDs exhibit extensive agglomeration, forming dense clusters with limited separation between particles. This morphology suggests strong interparticle interactions due to the high surface energy of the unmodified NDs. In contrast, the modified sample (Fig. 4b) displays a more dispersed distribution of ND clusters, indicating a significant reduction in agglomeration. The observed morphological changes suggest that surface functionalization with silane groups alters the surface energy and enhances the stability of the NDs in dispersion. These results confirm the effectiveness of the chemical modification in tailoring the surface properties of nanodiamonds, which is essential for improving their performance in composite materials or other applications requiring enhanced dispersibility and surface reactivity.

FTIR analysis

The FTIR spectrum of NDs modified with triethoxy(octyl)silane exhibits distinct absorption peaks that validate successful surface functionalization, as depicted in (Fig. 5). The strong absorption peaks observed at 2922 and 2854 cm^{-1} correspond to C–H stretching vibrations from the alkyl chains of the silane modifier, indicating the presence of octyl groups on the ND surface[44,45]. A prominent band at 1111 cm^{-1} is associated with Si–O–Si and Si–O–C stretching vibrations, confirming the formation of siloxane bonds resulting from hydrolysis and condensation reactions[46,47]. The peak around 1711 cm^{-1} may be related to O–H bending or the presence of adsorbed water[48,49]. Additional peaks at 913 cm^{-1} and 688 cm^{-1} are attributed to Si–C and Si–H stretching vibrations, respectively, further supporting the successful grafting of silane molecules[50–52]. Altogether, these

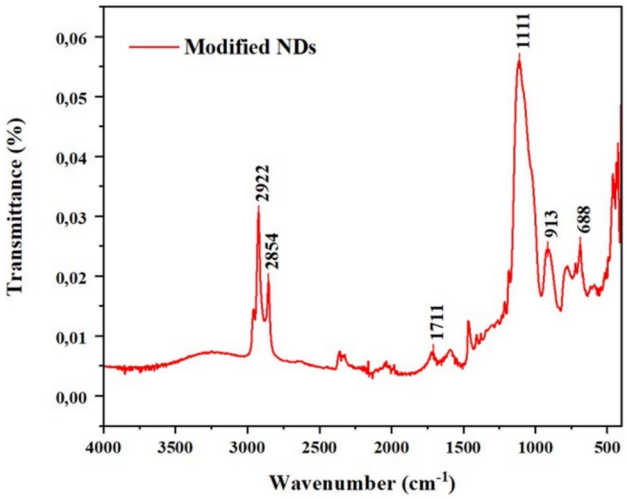

Fig. 5. FTIR patterns of the modified NDs.

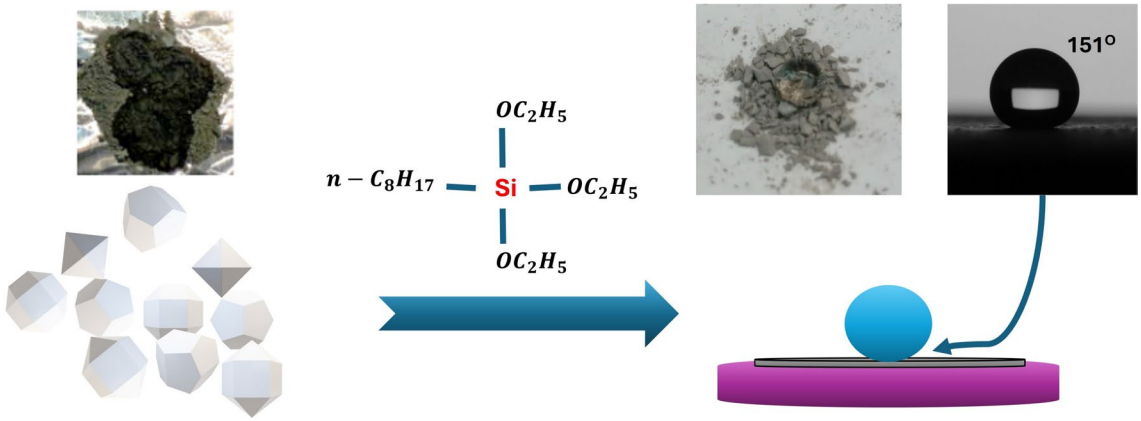

Fig. 6. Water contact angle (WCA) measurements of the modified NDs.

spectral characteristics affirm the effective modification of nanodiamonds with triethoxy(octyl)silane, enhancing their surface properties for potential applications.

Hydrophobicity analysis

The measurement of the water contact angle for ND surfaces coated with triethoxy(octyl)silane revealed a significant level of hydrophobicity, with a recorded angle of 151° based on more than five repeated measurements. This value categorizes the material as superhydrophobic compared to untreated ND powder, as shown in (Fig. 6). The consistency of this result indicates the effective attachment of hydrophobic silane groups, which drastically lower surface energy and restrict water spreading. Furthermore, the increased WCA may be influenced by nanoscale surface roughness resulting from ND aggregation, which facilitates the formation of air pockets that enhance water repellency, aligning with the Cassie–Baxter wetting model.

Enhancing hydrophobicity further could involve strategies such as increasing surface roughness through controlled ND clustering and optimizing silane functionalization to maximize the exposure of hydrophobic groups. These results demonstrate the potential of triethoxy(octyl)silane-modified NDs for use in applications requiring extreme water resistance, including waterproof coatings, self-cleaning surfaces, and anti-corrosion barriers.

DFT analysis of charge redistribution and hydrophobicity

To uncover how triethoxy(octyl)silane (TREOS) grafting turns nanodiamond (ND) from mildly hydrophilic to super-hydrophobic, we modelled three clusters: (i) pristine ND, (ii) TREOS-functionalized ND, and (iii) the same surface bearing one adsorbed H_2O molecule. All geometries were optimized at the B3LYP-D3/6–311 + + G (d, p) level.

Key structural changes

Silanisation leaves the diamond core intact but elongates C–C bonds at the attachment site by~ 0.01 Å, signaling electron withdrawal from surface carbons.

Charge of redistribution

Mulliken analysis (Fig. 7) shows that surface carbons shift from –0.02 e to –0.12 e after grafting, while Si (+ 1.18 e) and siloxane O atoms (–0.56 e) accommodate the lost charge. Electrostatic-potential (MEP) maps (Fig. 8) reveal that this rearrangement attenuates high-field regions on the ND surface by ≈ 40 kcalmol, effectively screening polar sites beneath the non-polar octyl chains.

Water adsorption

The functional layer suppresses hydrogen bonding: a single water molecule interacts weakly with the grafted surface ($E_{int} \approx -2$ kcal mol^{-1}; H···O > 3.2 Å), whereas it binds strongly to pristine ND ($E_{int} \approx -11$ kcal mol^{-1}; H···O ≈ 1.8 Å). The calculated trend mirrors the measured water-contact angle of 151°.

Practical implication

By lowering the surface free energy without compromising the diamond scaffold, TREOS grafting yields ND that disperses readily in non-polar matrices and retains hydrophobicity under humid conditions.

Conclusion

The successful functionalization of NDs with TREOS has been demonstrated through comprehensive structural, chemical, and surface characterization. The hydrolysis and condensation reactions effectively grafted silane molecules onto the ND surface, forming stable Si–O–C and Si–O–Si bonds. Characterization techniques, including XRD, scanning electron microscopy SEM, FTIR, and WCA measurements, confirmed the structural integrity of modified NDs and the presence of hydrophobic functional groups. The resulting superhydrophobicity, with a water contact angle of 151°, arises from the combined effects of nanoscale surface roughness and silane functionalization, which enhances water repellency. NDs have garnered significant interest due to their unique structural and chemical properties. Their small size, high surface area, and exceptional resilience make them promising materials for a wide range of applications. NDs can withstand extreme conditions without structural degradation, making them suitable for applications in energy conservation, biomedical devices, and advanced coatings. Their role as structural and functional materials extends to industries such as oil and gas, semiconductors, and surface engineering, where they are used for tool surface modification, grinding, and polishing. Further research will provide deeper insights into ND surface chemistry, unlocking new potential applications.

Although specific applications were not explored in this study, the hydrophobic NDs developed here hold promise for diverse uses. Potential applications include superhydrophobic coatings for anti-icing and self-cleaning surfaces, biocompatible hydrophobic composites for implants and drug delivery, and lubrication

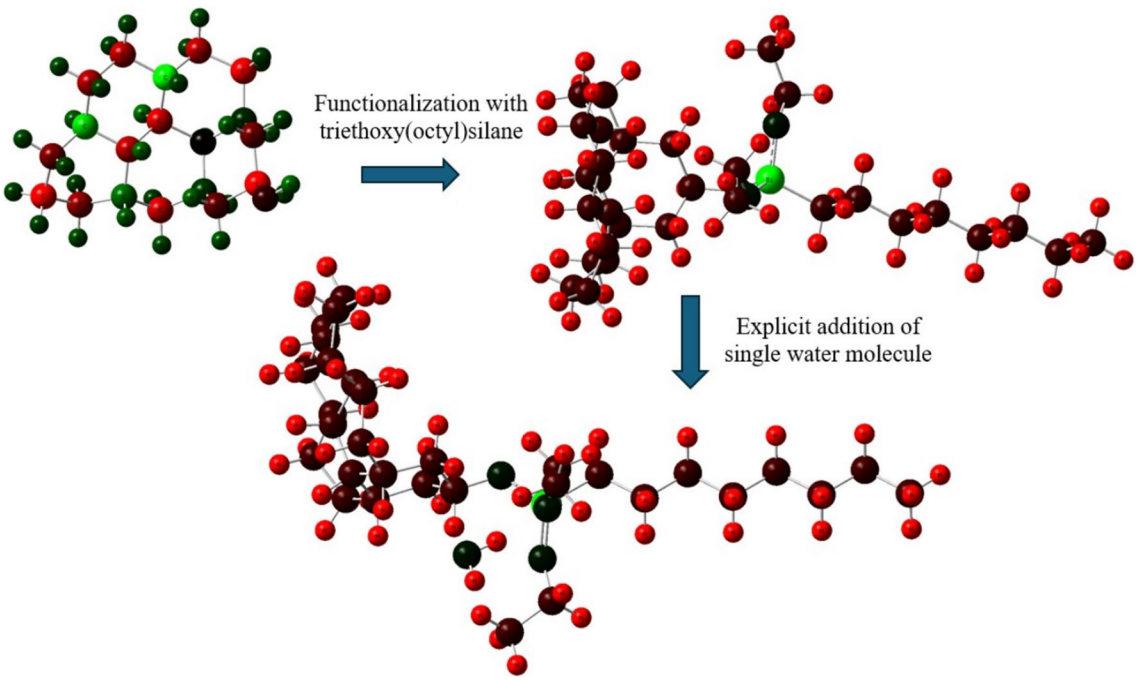

Fig. 7. Mulliken partial charges for key atoms in the three ND models. TREOS grafting drains electron density from surface carbons and concentrates it on Si/O, generating a buried dipole.

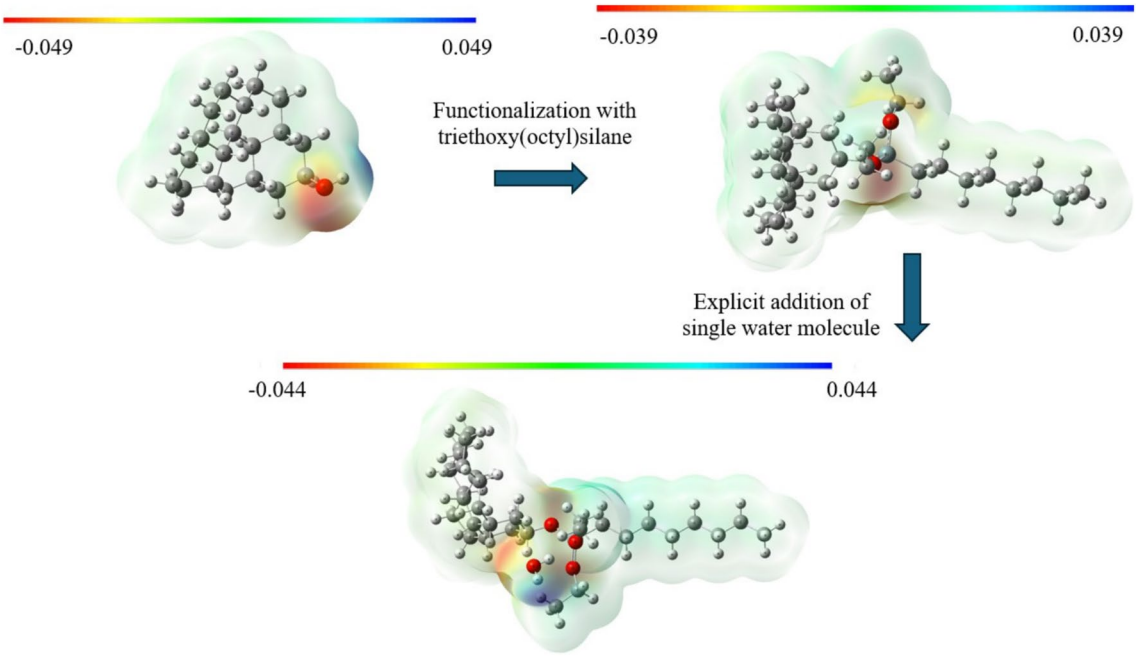

Fig. 8. Electrostatic-potential maps for (**a**) pristine ND, (**b**) TREOS-grafted ND, and (**c**) TREOS-grafted ND with an adsorbed H2O molecule. The common color scale (red = −40, blue = + 40 kcal mol − 1) highlights the loss of polar surface regions after functionalization.

or anti-wear properties through enhanced dispersion in nonpolar solvents. Future research should focus on integrating customized NDs into functional materials for real-world applications, such as protective coatings, biomedical devices, and advanced composites. This study establishes a foundation for further advancements in ND surface engineering, paving the way for broader industrial adoption.

Data availability

The datasets used and analysed during the current study are available from the corresponding author on reasonable request. All data generated or analysed during this study are included in this published article and its supplementary information files.

Received: 6 May 2025; Accepted: 1 July 2025
Published online: 07 July 2025

References

1. Krueger, A. et al. Deagglomeration and functionalisation of detonation diamond. *Phys. Status Solidi* **204**, 2881–2887 (2007).
2. Krueger, A. Beyond the shine: recent progress in applications of nanodiamond. *J. Mater. Chem.* **21**, 12571–12578 (2011).
3. Behler, K. et al. Nanodiamond-polymer composite. *ACS Nano* **3**, 363–369 (2009).
4. Alhaddad, A. et al. Corrigendum: nanodiamond as a vector for sirna delivery to ewing sarcoma cells. *Small* **7**, 3087 (2011).
5. Williams, O. et al. Growth, electronic properties and applications of nanodiamond. *Diam. Relat. Mater.* **17**, 1080–1088 (2008).
6. Korepanov, V. et al. Carbon structure in nanodiamonds elucidated from raman spectroscopy. *Carbon* **121**, 322–329 (2017).
7. Rangari, V., Mohammad, G., Jeelani, S., Butenko, Y. & Dhanak, V. Synthesis and characterization of diamond-coated cnts and their reinforcement in nylon-6 single fiber. *ACS Appl. Mater. Interfaces* **2**, 1829–1834 (2010).
8. Kausar, A. Nanodiamond nano-reinforcements in thermoplastic (polyamide, polyimide, polystyrene) nanocomposites—essential characteristics and technicalities. *J. Macromol. Sci. Part B* 1–26 (2024).
9. Thekkedath, A. & Sridharan, K. Nanodiamonds and its applications. In *IntechOpen eBooks* (eds Thekkedath, A. & Sridharan, K.) (IntechOpen, 2022).
10. Kumar, S. et al. Nanodiamonds: Emerging face of future nanotechnology. *Carbon* **143**, 678–699 (2019).
11. Hu, H., Guo, H., Yu, X., Naito, K. & Zhang, Q. Surface modification and disaggregation of detonation nanodiamond particles with biodegradable polyurethane. *Coll. Surf. A: Physicochem. Eng. Asp.* **563**, 302–309 (2018).
12. Toktarbaiuly, O., Kurbanova, A., Imekova, G., Abutalip, M. & Toktarbay, Z. Desert water saving and transportation for enhanced oil recovery: bridging the gap for sustainable oil recovery. *Eur. Chem. Technol. J.* **25**, 193–200 (2023).
13. Seralin, A., Sugurbekova, G., Kurbanova, A., Nuraje, N. & Toktarbaiuly, O. Designing water-repellent concrete composites using cheap organic materials. *Eur. Chem. J.* **24**, 251–258 (2022).
14. Suiindik, Z. et al. Formulating superhydrophobic coatings with silane for microfiber applications. *Eur. Chem. J.* **26**, 53–60 (2024).
15. Kydyrbay, N. et al. Enhancing road durability and safety: a study on silica-based superhydrophobic coating for cement surfaces in road construction. *Eng. Sci.* **39**, 1221 (2024).
16. Kurbanova, A. et al. Superhydrophobic sio_2/trimethylchlorosilane coating for self-cleaning application of construction materials. *Coatings* **12**, 1–9 (2022).
17. Liu, R. et al. Synthesis of biopolymer-grafted nanodiamond by ring-opening polymerization. *Diam. Relat. Mater.* **50**, 26–32 (2014).
18. Barras, A., Lyskawa, J., Szunerits, S., Woisel, P. & Boukherroub, R. Direct functionalization of nanodiamond particles using dopamine derivatives. *Langmuir* **27**, 12451–12457 (2011).

19. Zhang, X. et al. Polymer-functionalized nanodiamond platforms as vehicles for gene delivery. *ACS Nano* **3**, 2609–2616 (2009).
20. Zhou, Y. et al. Preparation of superhydrophobic nanodiamond and cubic boron nitride films. *Appl. Phys. Lett.* **97**, 133110 (2010).
21. Uzoma, P. et al. Anti-bacterial, icephobic, and corrosion protection potentials of superhydrophobic nanodiamond composite coating. *Coll. Surf. A: Physicochem. Eng. Asp.* **630**, 127532 (2021).
22. Petkov, V. & Valov, R. Structure and morphology of composite coating of chromium with diamond nanoparticles on sintered steels. *SN Appl. Sci.* **1**, 1546 (2019).
23. Chevallier, E., Scorsone, E. & Bergonzo, P. New sensitive coating based on modified diamond nanoparticles for chemical saw sensors. *Sens. Actuat. B Chem.* **154**, 238–244 (2011).
24. Wei, L. & Yushin, G. Nanostructured activated carbons from natural precursors for electrical double-layer capacitors. *Nano Energy* **1**, 552–565 (2012).
25. Liu, Y. & Kim, D. Enhancement of capacitance by electrochemical oxidation of nanodiamond-derived carbon nano-onions. *Electrochim. Acta* **139**, 82–87 (2014).
26. Miele, E. et al. Controlling wetting and self-assembly dynamics by tailored hydrophobic surfaces. *Adv. Mater.* **26**, 4179–4183 (2014).
27. Baptisa, F., Belhout, S., Giordani, S. & Quinn, S. Recent developments in carbon nanomaterial sensors. *Chem. Soc. Rev.* **44**, 4433–4453 (2015).
28. Simoni, N., Silva, T., Oliveira, G. & Fatbello-Filho, O. A nanodiamond-based electrochemical sensor for the determination of pyrazinamide antibiotic. *Sens. Actuat. B Chem.* **250**, 315–323 (2017).
29. Jiang, L., Nelson, G., Abda, J. & Foord, J. Novel modifications to carbon-based electrodes to improve the electrochemical detection of dopamine. *ACS Appl. Mater. Interfaces* **8**, 26338–28348 (2016).
30. Mochalin, V., Shenderova, O., Ho, D. & Gogotsi, Y. The properties and applications of nanodiamonds. *Nat. Nanotechnol.* **7**, 11–23 (2012).
31. Zhong, Y., Loh, K., Midya, A. & Chen, Z. Suzuki coupling of aryl organics on diamond. *Chem. Mater.* **20**, 3137–3144 (2008).
32. Krysoca, H. et al. Dye sensitization of boron-doped diamond foam: Champion photo electrochemical performance of diamond electrodes under solar light illumination. *RSC Adv.* **5**, 81069–81077 (2015).
33. Tafti, M. & Sadeghzadeh, S. Novel use of nanodiamonds as a light-scattering material in dye-sensitized solar cells. *J. Mater. Sci. Mater. Electron.* **27**, 5225–5232 (2016).
34. Ansari, S. et al. Role of nanodiamonds in drug delivery and stem cell therapy. *Iran. J. Biotechnol.* **14**, 130 (2016).
35. Frisch, M. et al. *Gaussian 09, revision a.02* (Gaussian Inc, 2016).
36. Lu, T. & Chen, F. Multiwfn: A multifunctional wavefunction analyzer. *J. Comput. Chem.* **33**, 580–592 (2012).
37. Humphrey, W., Dalke, A. & Schulten, K. Vmd: visual molecular dynamics. *J. Mol. Graph.* **14**, 33–38 (1996).
38. Gill, P., Johnson, B., Pople, J. & Frisch, M. The performance of the becke—lee—yang—parr (b—lyp) density functional theory with various basis sets. *Chem. Phys. Lett.* **197**, 499–505 (1992).
39. Baranov, O., Komarova, L. & Golubkov, S. Hydrophobic coatings based on triethoxy(octyl)silane. *Russ. Chem. Bull.* **69**, 1165–1168 (2020).
40. Salon, M. & Belgacem, M. Hydrolysis-condensation kinetics of different silane coupling agents. *Phosphorus, Sulfur Silicon Relat. Elem.* **186**, 240–254 (2011).
41. Khachatryan, A. et al. Graphite-to-diamond transformation induced by ultrasound cavitation. *Diam. Relat. Mater.* **17**, 931–936 (2008).
42. Ferrari, A. & Robertson, J. Raman spectroscopy of amorphous, nanostructured, diamond-like carbon, and nanodiamond. *Philos. Trans. A Math. Phys. Eng. Sci.* **362**, 2477–2512 (2004).
43. Prawer, S. et al. The raman spectrum of nanocrystalline diamond. *Chem. Phys. Lett.* **332**, 93–97 (2000).
44. Light, U. et al. Nanomaterials. *Nanomaterials* **5**, 11 (2021).
45. Piryantiki, Y., Dolgov, L. & Yaroshchuk, O. Condensed matter spectroscopy. *Condens. Matter Spectrosc.* **108**, 1 (2010).
46. Kayahan, E. Unspecified title. *J. Lumin.* **130**, 1295 (2010).
47. Ben Slama, S., Hajji, M. & Ezzaouia, H. Unspecified title. *Nanoscale Res. Lett.* **7**, 1 (2012).
48. Martín, R., Heydorn, P., Alvaro, M. & Garcia, H. General strategy for high-density covalent functionalization of diamond nanoparticles using fenton chemistry. *Chem. Mater.* **21**, 4505–4514 (2009).
49. Girard, H. et al. Surface properties of hydrogenated nanodiamonds: a chemical investigation. *Phys. Chem. Chem. Phys.* **13**, 11517–11523 (2011).
50. Aurilio, M. & Baaj, H. Examining the effects of a self-healing elastomer on the properties of bitumen. In *Proceedings of the RILEM International Symposium on Bituminous Materials: ISBM Lyon 2020 1*, 857–863 (Springer, 2022).
51. Chen, C. & Chen, Y. Unspecified title. *Appl. Phys. Lett.* **75**, 2560 (1999).
52. Sun, J., Lu, Y., Du, X. & Kulinich, S. Unspecified title. *Appl. Phys. Lett.* **86**, 1 (2005).

Acknowledgements

The authors gratefully acknowledge the support provided by the Ministry of Science and Higher Education of the Republic of Kazakhstan through Grant No. AP19679222. They also extend their appreciation to the Targeted Program of the MHES of the Republic of Kazakhstan for its assistance under Grant No. BR21882439.

Author contributions

N.K.: Writing—review & editing, Writing—original draft, Software, Methodology, Investigation, Data curation, Conceptualization. M. Z: Writing—review & editing, Methodology, Investigation, Software. M.A.: Writing—review & editing, Resources. T.D.: Software, Formal analysis. Y.T.: Investigation, Data curation. A.A and M.K.: Software, Data curation. N.N.: Supervision, Conceptualization. O.T.: Writing—review & editing, Supervision, Project administration, Funding acquisition, Conceptualization.

Declarations

Competing interests

The authors declare no competing interests.

Additional information

Correspondence and requests for materials should be addressed to O.T.

Reprints and permissions information is available at www.nature.com/reprints.